References

BIANCHI, R., PILATI, T. & SIMONETTA, M. (1978). *Acta Cryst.* B**34**, 2157-2162.

COCHRAN, W. (1955). *Acta Cryst.* **8**, 473-478.

DECLERCQ, J. P., GERMAIN, G. & VAN MEERSSCHE, M. (1972). *Cryst. Struct. Commun.* **1**, 13-15.

FISKE, S. J. (1982). DPhil Thesis, Univ. of York.

HULL, S. E. & IRWIN, M. J. (1978). *Acta Cryst.* A**34**, 863-870.

HULL, S. E., LEBAN, I., WHITE, P. S. & WOOLFSON, M. M. (1976). *Acta Cryst.* B**32**, 2374-2381.

KARLE, J. & HAUPTMAN, H. (1956). *Acta Cryst.* **9**, 635-651.

SAYRE, D. (1952). *Acta Cryst.* **5**, 60-65.

YAO JIA-XING (1981). *Acta Cryst.* A**37**, 642-644.

Acta Cryst. (1985). A**41**, 290-296

Reflectivity (Rocking) Curves of Imperfect Crystals by an Improved $\Delta\omega$, $\Delta 2\theta$ Technique

BY A. MCL. MATHIESON AND A. W. STEVENSON

Division of Chemical Physics, CSIRO, PO Box 160, *Clayton, Victoria, Australia* 3168

(*Received* 7 *September* 1984; *accepted* 19 *December* 1984)

Abstract

A simple experimental modification to the $\Delta\omega$, $\Delta 2\theta$ technique for measuring single-crystal Bragg reflections has been demonstrated [Mathieson & Stevenson (1984). *Aust. J. Phys.* **37**, 657-665]. This leads to a significant improvement in this technique in that the source component is reduced to a minor (angular) role, so that the greater resolution-capability/information-content, inherent in the $\Delta\omega$, $\Delta 2\theta$ method relative to the conventional $\Delta\omega$ profile method, is further enhanced. With only two major components in the two-dimensional distribution, the individual distributions of these components can be determined with some accuracy. These components are the reflectivity (often referred to previously as the mosaic spread) and the wavelength distribution. The resolution function, $R(\Delta\omega, \Delta 2\theta)$, can be estimated from the experimental parameters and is sufficiently small that the deconvoluted reflectivity for imperfect crystals is derivable. This procedure is demonstrated, in the present case, for a small single crystal of $CuInSe_2$.

1. Introduction

The basic design of the single-crystal X-ray diffractometer was established by Bragg (1914). In essence, it has not changed a great deal nor has the measurement procedure associated with it. This procedure involves traversing a single reflection by changing the orientation of the specimen crystal, step by step, and recording, at each step, $\Delta\omega$, the diffracted intensity passed through a relatively wide aperture in front of the detector, thereby providing the one-dimensional intensity profile, $I(\Delta\omega)$, of the reflection. The main purpose of the original instrument was the estimation of the integrated intensity, $\int I(\Delta\omega)\,\mathrm{d}\Delta\omega$.

For several decades, this instrument was overshadowed by photographic recording, using effectively a very large (or no) aperture. Then, in the 1950's, the X-ray diffractometer was resurrected as an instrument for quantitative measurements on small single crystals (see Arndt & Willis, 1966), and Alexander & Smith (1962) carried out an analysis of the relationship of the profile curve $I(\Delta\omega)$ to what they nominated as the various major components of the experiment. They assumed the probable functional form, in terms of the one variable $\Delta\omega$, of a number of components, the mosaic spread, μ, the source size, σ, the wavelength distribution, λ, and the specimen-crystal size, c. The theoretical intensity curve, $I(\Delta\omega)_{\mu,\sigma,\lambda,c}$, was derived by sequential convolution of the functions. In this analysis, however, there was one component whose parametric relevance was largely ignored, namely the aperture in front of the detector. The variation of signal distribution across the aperture, $I(\Delta 2\theta)$, for a given value of $\Delta\omega$, was not examined or explored, only the outer limits necessary to ensure collection of the total signal within the specimen scan limits were investigated ('minimum receiving aperture'). Hence, what is measured under the circumstances of the conventional procedure is detailed in (1):

$$I(\Delta\omega)_{\mu,\sigma,\lambda,c,A(\Delta 2\theta)} = \int_{\Delta 2\theta_1}^{\Delta 2\theta_2} I(\Delta\omega, \Delta 2\theta)_{\mu,\sigma,\lambda,c}\,\mathrm{d}\Delta 2\theta, \quad (1)$$

and it is evident that one is really dealing with a five-component system in which the square-wave function, $A(\Delta 2\theta)$, corresponding to the aperture, is the largest component, in angular terms, by the nature of the determination of its outer limits.

The main aim of the analysis by Alexander & Smith (1962) was directed at measuring relative integrated intensities with high reliability. If, however, one wishes to use the diffractometer to extract, from such one-dimensional intensity measurements, informa-

0108-7673/85/030290-07$01.50

tion on matters other than integrated intensity, say, the mosaic spread, $\mu(\Delta\omega)$, a physical quantity that is specimen specific, there are considerable difficulties. The function sought is generally one of the smaller of those components that, convoluted together, reproduce the profile distribution, $I(\Delta\omega)$, and, hence, because of its relative size, is virtually impossible to extract by deconvolution procedures from normal diffractometer measurements. Under these circumstances, physical modification of the specimen is necessary to increase the range of $\mu(\Delta\omega)$ so that it becomes the dominant component and is then extractable by mathematical procedures. However, such modification may not be advisable or even feasible and it then becomes necessary to consider the problem *ab initio*.

When dealing with an experiment involving several components, the restriction to one-dimensional measurement is obviously a severe one, particularly when, as noted above, the component of greatest physical significance, the mosaic spread, μ, is likely to be a relatively minor component (major and minor in terms of angular range). There is an obvious advantage to be gained in defining the experimental situation more rigorously by either reducing the number of major components or by increasing the number of measurement parameters (variables) or both.

The first experimental exploration of the intensity distribution, $I(\Delta\omega, \Delta 2\theta)$ (Mathieson, 1982), using a narrow aperture in front of the detector, corresponded to an increase in the number of measurement parameters. The increased information content derived with the additional parameter was immediately obvious in that the individual major components were readily identified by their characteristic loci (or slopes) in $\Delta\omega, \Delta 2\theta$ space. There was, in effect, a form of partial deconvolution. Preliminary estimates of the three principal components, μ, σ, λ, could be obtained by slice scans (Mathieson, 1982) while additional precision could be envisaged by generating synthetic distributions, $I_{\rm calc}(\Delta\omega, \Delta 2\theta)$, from these preliminary estimates and refining against the experimental distribution. A theoretical study has been presented (Mathieson, 1984*a*), which stresses the intimate relationship between μ and the 'level of interaction' (Mathieson, 1979) or reflectivity, r, and hence the vital importance of deriving an accurate estimate of this particular component distribution. From this point on, this distribution will be referred to as μ/r (or r/μ).

While the $\Delta\omega, \Delta 2\theta$ approach opens up the measurement situation and points to the possibility of deriving accurate estimates of μ/r, the situation is still relatively complex in that three major components remain and, in addition, there are minor components, such as crystal size, c (Mathieson, 1984*b*), whose presence would degrade the accuracy of a deconvolution process based on the three major components alone. Again, it is clear that a change to bring the component/parameter ratio nearer to unity would be valuable.

To this end, we have recently arrived at an improved experimental technique (Mathieson & Stevenson, 1984) by which the effective size of the source, in the diffraction plane, from a standard X-ray tube, normally a major component, can be reduced markedly without significant loss of peak intensity in the $I(\Delta\omega, \Delta 2\theta)$ distribution. This means that there are only two principal components, μ/r and λ, remaining in $\Delta\omega, \Delta 2\theta$ space and their individual distributions can therefore be determined more directly and more accurately. In addition, the minor components previously buried in the distribution associated with three major components begin to emerge and are more readily identified.

To illustrate the capabilities of the improved technique, an example concerning the derivation of a reflectivity curve is presented. To assist in the presentation, for this and other examples, it is first necessary to summarize the properties of $\Delta\omega, \Delta 2\theta$ space and of affine transformations since these facilitate use of that space.

2. $\Delta\omega, \Delta 2\theta$ space

The space we are concerned with is the local region adjacent to a Bragg reflection where the component parameters are essentially linear. Conventionally, Bragg reflections are dealt with in terms of reciprocal space, *e.g.* in discussing the resolution function, *cf.* Cochran (1969), but, for our purposes, there are disadvantages in that viewpoint, as we indicate below.

Let us consider, first, the situation in reciprocal space in respect of two reciprocal-lattice points interacting with the Ewald circle, one at a low θ angle and the other at a high θ angle, Figs. 1(*a*)(i) and (ii) respectively. The loci of the components μ, σ, λ and the detector parameter $\Delta 2\theta$ are indicated. Appropriately oriented and on an enlarged but the same scale, these two cases are depicted in Figs. 1(*b*)(i) and (ii) respectively to facilitate comparison of the disposition of the loci. These figures demonstrate the way in which the dimensions of the components μ, σ, λ all change with θ, being proportional to d^*, with an extra $\tan\theta$ scale expansion for λ and also how the relative dispositions of the loci change with θ.

On the other hand, when we view the local space adjacent to the Bragg reflection for these two cases in terms of simple angular measure, Figs. 1(*c*)(i) and (ii), then μ, σ and $\Delta 2\theta$ do not change with θ nor does the relative disposition of the loci (see also Mathieson, 1983*a*). Only λ changes dimensionally with θ, but in a well established manner. Because of these features, there are, for ease of comparison of reflections at different θ angles and for the detection of the minor differences between them, obvious

advantages in dealing in terms of the local angular measure, and we have chosen in practice to deal in terms of the operational angular variables $\Delta\omega$ and $\Delta 2\theta$, the specimen local angular movement and what we may refer to as the detector angular dimension space respectively.

With a two-dimensional array of measurements (data points), one can carry out various transformations so that the various components may be more readily recognized, appreciated or measured. The possibilities of such transformations are discussed in § 3.

3. Affine transformations

The variable $\Delta 2\theta$ lies along the Ewald circle and, for the limited region adjacent to the point P [Fig. 1(*a*)], is effectively linear and tangential to the circle at that point. It therefore corresponds to the displacement across the conventional wide aperture. Hence it follows that, when one considers a scan mode $\omega/s\theta$ (Mathieson, 1983*a*, *b*), what one does in the classical viewpoint when moving the specimen crystal from $\Delta\omega_m$ to $\Delta\omega_{m+1}$ is to displace the detector aperture along $\Delta 2\theta$ by $+s\Delta\omega$. In the $\Delta\omega$, $\Delta 2\theta$ viewpoint, this corresponds to displacing the line of $\Delta 2\theta$ data points for $\Delta\omega_{m+1}$ by $-s\Delta\omega$ relative to the line of $\Delta 2\theta$ data points for $\Delta\omega_m$ since one is moving the detector frame of reference relative to the diffraction distribution. In other words, the scan procedure corresponds to an affine transformation parallel to one axis, the $\Delta 2\theta$ axis. It is useful to summarize the effect of such transformations on the mutual orientation of the components and their relation to the operational parameters.

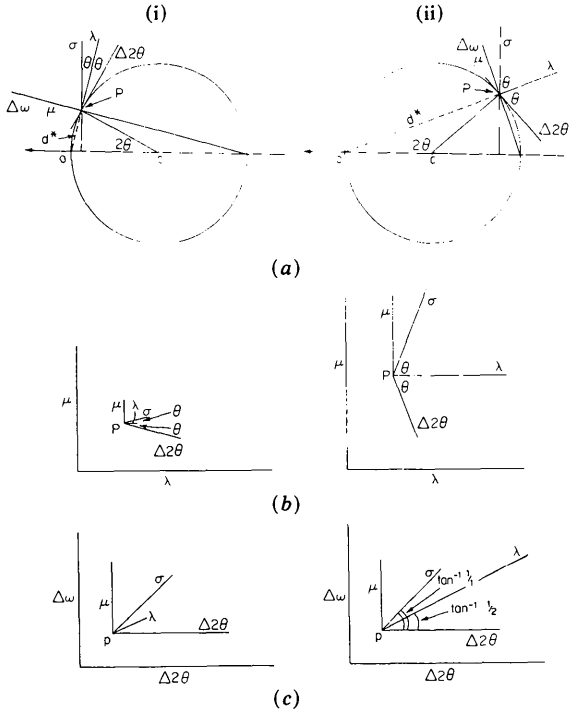

Fig. 1. Comparison of (i) low-θ and (ii) high-θ reflections. (*a*) The Ewald-circle construction for diffraction at a point P associated with a vector d^* in reciprocal space. The angular variables $\Delta\omega$, $\Delta 2\theta$ and the components μ, σ, λ are identified. (*b*) These diagrams reproduce on an enlarged scale the details around point P from Figs. 1(*a*)(i) and (ii) respectively. They show how, in reciprocal space, the components μ, σ, λ change both their size and mutual disposition with change in θ. (*c*) The relationships between the components μ, σ, λ and the angular variables in $\Delta\omega$, $\Delta 2\theta$ space. The invariance of the mutual disposition of the components μ, σ, λ and the angular variables $\Delta\omega$, $\Delta 2\theta$ is demonstrated as is the dimensionality of the components μ, σ. The only one of these components varying intrinsically with θ is λ, whose length is proportional to tan θ.

(a) Displacement parallel to $\Delta 2\theta$

In mathematical terms, this class of displacement can be represented by $\Delta\omega^{(s)} = \Delta\omega^{(0)}$ and $\Delta 2\theta^{(s)} = \Delta 2\theta^{(0)} - s\Delta\omega^{(0)}$. $s = 0$ corresponds to the ω scan, $s = 1$ to the ω/θ scan and $s = 2$ to the $\omega/2\theta$ scan, Figs. 2(*a*)(i), (ii) and (iii) respectively. The changes that occur in respect of the components μ, σ, λ are depicted in Fig. 2(*a*), that for the crystal size, c (Mathieson, 1984*b*), being included for completeness. The latter, unlike the first three, changes the slope of its locus with change in θ. It has already been pointed out (Mathieson, 1983*a*) that the $s = 1$ transformation [Fig. 2(*a*)(ii)] provides a representation that is reciprocal-lattice compatible.

This viewpoint provides a useful physical picture of the relationship between scan modes and how, for each scan mode, the various components line up with respect to the $\Delta 2\theta$ axis. It can aid in avoiding misinterpretations that can creep in when one's viewpoint is restricted to a purely one-dimensional one (see Mathieson, 1983*c*).

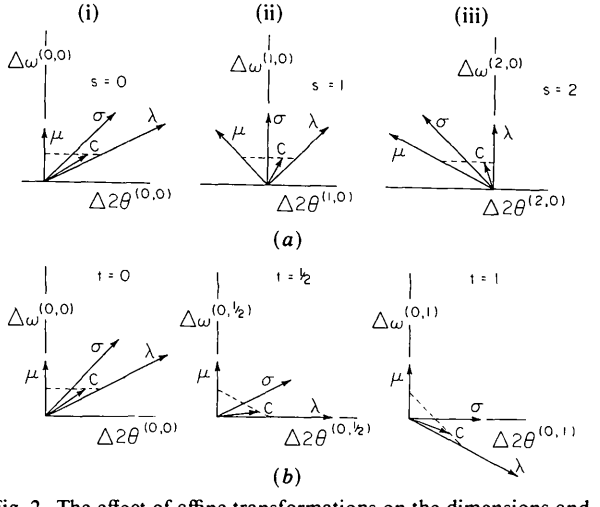

Fig. 2. The effect of affine transformations on the dimensions and mutual dispositions of the components μ, σ, λ in $\Delta\omega^{(s,t)}$, $\Delta 2\theta^{(s,t)}$ space. (*a*) The effect of displacements parallel to the $\Delta 2\theta$ axis for (i) $s = 0$, (ii) $s = 1$ and (iii) $s = 2$. (*b*) The effect of displacements parallel to the $\Delta\omega$ axis for (i) $t = 0$, (ii) $t = 1/2$ and (iii) $t = 1$.

(*b*) *Displacement parallel to* $\Delta\omega$

In mathematical terms, this class of displacement can be represented by $\Delta\omega^{(t)} = \Delta\omega^{(0)} - t\Delta 2\theta^{(0)}$ and $\Delta 2\theta^{(t)} = \Delta 2\theta^{(0)}$.

This type of transformation has no obvious function in relation to the classical wide-aperture procedure since it involves associating $\Delta 2\theta$ data points from different $\Delta\omega$ settings. It is only with a two-dimensional $\Delta\omega$, $\Delta 2\theta$ array of data points that transformations of this type are feasible.

For illustration, we consider only three possibilities here, $t = 0$, $t = 1/2$ and $t = 1$, Figs. 2(*b*)(i), (ii) and (iii) respectively. That for $t = 1/2$, Fig. 2(*b*)(ii), is of interest in that it provides a form of presentation that is readily related to a reciprocal-space-compatible one, see Figs. 1(*b*)(i) and (ii). Fig. 2(*b*)(ii) is in angular measure and the $\sigma\lambda$ angle is $\tan^{-1} 1/2$ and invariant with θ. If the component σ is reduced to a minor status relative to μ and λ, then, in such a two-component two-dimensional distribution where μ/r and λ are at right angles, the estimation of these components, individually, is feasible.

When two non-zero affine transformations (s, t) are applied to a two-dimensional ($\Delta\omega$, $\Delta 2\theta$) array in respect of two axes, the operations are non-commutative and the sequence of operations must be defined.

4. Measurement of the 'level of interaction' (reflectivity)/mosaic distribution for a single reflection

In terms of an ideal experiment, what one seeks to achieve is the measurement of the reflectivity distribution of any given reflection of the specimen crystal, with radiation of an infinitely narrow waveband from a vanishingly small source, the measurements being preferably placed on an absolute scale by reference to the incident beam. Then $I(\Delta\omega) \propto r(\Delta\omega)$, where $r(\Delta\omega)$ is the reflectivity (see Mathieson, 1984*a*).

However, in the practical terms of the majority of the experimental arrangements that have been devised to investigate Bragg reflections from small single crystals, this core information about reflectivity is smeared out and obscured by the convoluting operation of the many other components introduced as part of the experimental set-up to obtain measurable diffracted intensity, as outlined in § 1.

We may summarize this situation, in respect of the classical conventional measurement procedure, by the generalized relationship in (2):

$$I(\Delta\omega) \propto r(\Delta\omega) * R(\Delta\omega), \qquad (2)$$

where I is the measured intensity and R the resolution or instrument function. For imperfect crystals, the more appropriate symbol for the reflectivity would be r^*, the extinguished reflectivity distribution.

To disentangle the information concerning the reflectivity distribution $r^*(\Delta\omega)$ for small imperfect crystals from the measurements of the intensity profile $I(\Delta\omega)$ is an almost insurmountable task. The various components of the one-dimensional resolution function $R(\Delta\omega)$, namely σ, λ, A *etc.*, are, in angular terms, either singly and certainly together, of so much greater (angular) magnitude than r^* that the inverse process of deconvoluting r^* from I is virtually impossible.

There are two ways of tackling this fundamental problem. One is to increase the angular range of $r^*(\Delta\omega)$, *i.e.* to increase the angular range of the mosaic spread of the specimen so that it is significantly greater than that of the resolution function, $R(\Delta\omega)$, and deconvolution may be feasible. This classical solution (in the extreme - powdering the specimen - see Darwin, 1922, p. 826) has been used more recently by Schneider, Hansen & Kretschmer (1981) in γ-ray diffraction and by Yelon, van Laar, Kaprzyk & Maniawski (1984) in neutron diffraction. This approach may involve increasing the mosaic spread to a FWHH of many minutes of arc. It does mean that one is modifying the specimen significantly and such an approach may not be feasible in all cases, *e.g.* brittle materials. Also, one may wish to investigate a given specimen without modification.

The other approach is to reduce the angular range of R. $R(\Delta\omega)$ has many components (see above), the one with the most significant effect on $I(\Delta\omega)$ being generally the wide aperture in front of the detector in the conventional procedure. When a narrow aperture is substituted, then the measurement situation is two dimensional and the angular resolution is greatly improved, so that one can begin to recognize the individual contributing components μ, σ, λ and can attempt to determine their individual (angular) magnitudes (see Mathieson, 1984*a*). Here, the resolution function becomes two dimensional, $R(\Delta\omega, \Delta 2\theta)$.

It is then obvious that the further reduction of the number of principal components to two and so to the same number of dimensions as $\Delta\omega$, $\Delta 2\theta$ space is a highly advantageous step, see Figs. 2 and 6 in Mathieson (1984*a*). In the case treated here, the effective source size in the diffraction plane has been reduced to the order of 50 μm (equivalent on our Picker diffractometer to *ca* 0·01° (or 40″) in terms of $\Delta\omega$) (Mathieson & Stevenson, 1984) so that one should be able to derive useful information in a relatively direct manner concerning mosaic spreads with a FWHH of a few hundredths of 1° and certainly differentiate between, say, Gaussian and Lorentzian distributions.

When there are only two major components, such as r^* and λ, the relationship with the intensity distribution is given, for example, by (3):

$$I(\Delta\omega^{(0,1/2)}, \Delta 2\theta^{(0,1/2)}) \propto [r^*(\Delta\omega^{(0,1/2)}) \times \lambda(\Delta 2\theta^{(0,1/2)})] * R(\Delta\omega^{(0,1/2)}, \Delta 2\theta^{(0,1/2)}), \qquad (3)$$

where we have considered the $s=0$, $t=1/2$ case [*cf.* Fig. 2(*b*)(ii)], and R is the resolution function, containing σ, A *etc.*, but not λ (the λ component being readily identified in $\Delta\omega$, $\Delta 2\theta$ space).

In operational terms, the $I(\Delta\omega, \Delta 2\theta)$ ($s=0$) distribution, Fig. 3(*a*),† is transformed to a representational form that allows convenient extraction of the reflectivity distribution. This can be achieved by an affine transformation of the type $t=1/2$ [Fig. 3(*b*)(i)]. Provided the mosaic distribution of the specimen crystal is homogeneous along the crystal, then, over the wavelength band, say an α_1, α_2 doublet, the r^* distribution is generally invariant (see Mathieson, 1984*a*) so summation parallel to the λ axis [see Fig. 2(*b*)(ii)] will yield the distribution, Fig. 3(*c*).

An alternative approach is to transform the data array to the $s=2$, *i.e.* $\omega/2\theta$ scan mode [Fig. 3(*b*)(ii)] (see also Mathieson, 1983*d*). In this case, the vertical axis is λ while the μ/r axis is at a slope of $-\tan^{-1} 1/2$ to the $\Delta 2\theta$ axis. By summing parallel to the λ axis and over the same $\Delta\lambda$ waveband,‡ one can derive the one-dimensional distribution $r^*(\Delta 2\theta)$. The resultant distribution should, of course, be essentially independent of the size of the $\Delta\lambda$ waveband, but the step in $\Delta 2\theta$ is twice that in $\Delta\omega$. In practice, the resulting curve was, as expected, virtually identical to that in Fig. 3(*c*).

The FWHH of the reflectivity distribution in Fig. 3(*c*) is ~2′. The technique outlined here is one that does not necessitate complex equipment and can be readily set up with existing conventional diffractometers. Nevertheless, its capability in respect of imperfect crystals is compatible with more elaborate set-ups, *e.g.* using a γ-ray source, Yelon *et al.* (1981) on HgI_2 and Loshmanov *et al.* (1984) on ZnO. It is interesting to note that a slice scan (Mathieson, 1982) taken parallel to the μ axis for the two-dimensional array of data points, collected with a 'short' source instead of a 'tall' source (Mathieson & Stevenson, 1984) and transformed according to $s=2$, has a shape similar to that in Fig. 3(*c*) and a FWHH of ~2·5′. This slice scan was taken on the low-wavelength side of the α_1 peak so that there would be no corruption due to the σ component associated with the α_2 peak. It would seem that such a scan would provide an adequate starting point, for μ, in the synthesis of the various components, with a view to modelling the observed intensity distribution $I(\Delta\omega, \Delta 2\theta)$ (see § 1). If the two-dimensional array of data points is used to derive a distribution analogous to Fig. 3(*c*) the

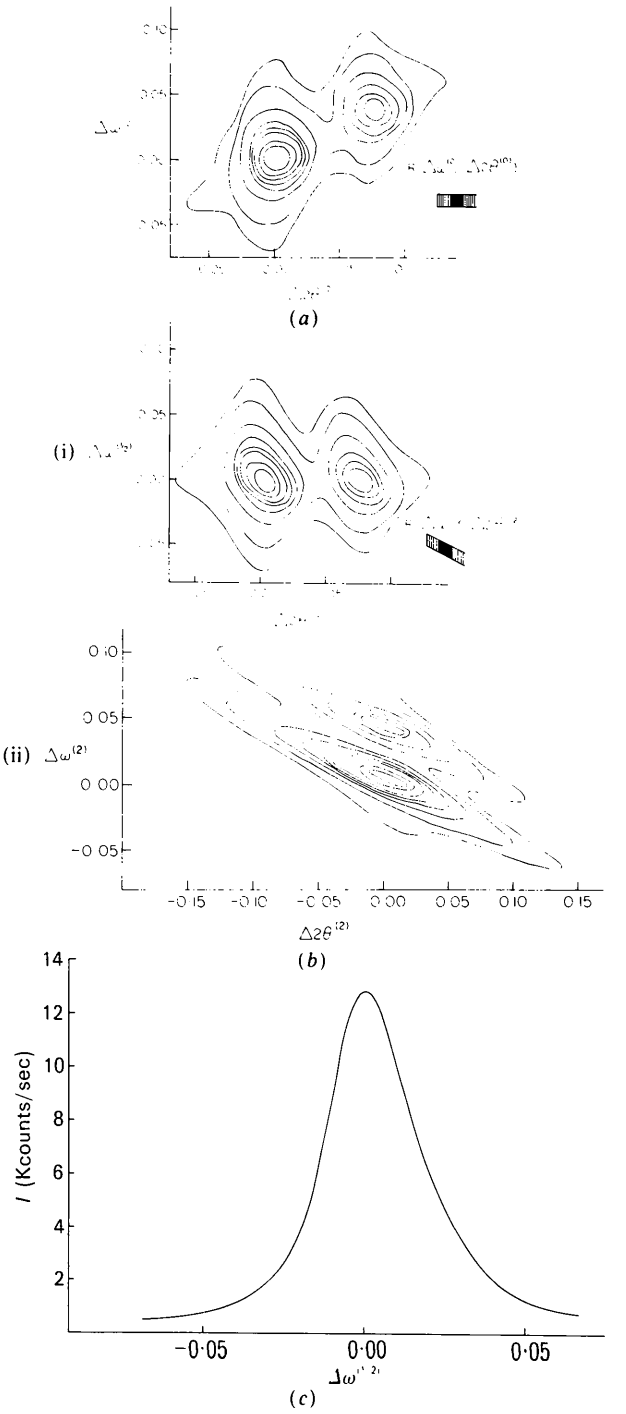

Fig. 3. (*a*) $I(\Delta\omega, \Delta 2\theta)$ ($s=0$) distribution obtained for the $\bar{1}\bar{1}2$ reflection of $CuInSe_2$ with Mo $K\alpha$ radiation. The resolution function, $R(\Delta\omega^{(0)}, \Delta 2\theta^{(0)})$, is estimated by convoluting the distributions associated with the source size (~0·01° along both $\Delta\omega^{(0)}$ and $\Delta 2\theta^{(0)}$) and the detector aperture size (~0·02° along $\Delta 2\theta^{(0)}$). (*b*) The result, for the $I(\Delta\omega, \Delta 2\theta)$ distribution depicted in (*a*), of applying an affine transformation according to (i) $t=1/2$ and (ii) $s=2$. The resolution function, $R(\Delta\omega^{(1/2)}, \Delta 2\theta^{(1/2)})$, is an appropriate modification of $R(\Delta\omega^{(0)}, \Delta 2\theta^{(0)})$. (*c*) The extinguished reflectivity distribution, $r^*(\Delta\omega)$, derived by summing data points parallel to the λ axis of Fig. 3(*b*)(i) [see Fig. 2(*b*)(ii)].

† Fig. 3(*a*) was obtained for the $\bar{1}\bar{1}2$ reflection of a small single crystal (average dimension ~0.06 mm) of tetragonal $CuInSe_2$, using a 'tall' source (Mathieson & Stevenson, 1984) of unfiltered Mo $K\alpha$ radiation. The θ value for this reflection is ~6.1°.

‡ One might more conveniently carry out this procedure after further transforming the data array according to $t=-1/2$, so that the λ and μ/r axes are at right angles.

result is a much broader curve (FWHH ~ 3·5′) owing to the larger contribution of σ.

The reflectivity distribution derived in Fig. 3(*c*) is still convoluted with the remaining resolution or instrument function, or, rather, its component parallel to $\Delta\omega$, the resolution function being $R(\Delta\omega, \Delta 2\theta)$. This, however, is now quite small and may be determined either by estimation based on the size of the source and the size of the detector aperture (see Appendix), as in Figs. 3(*a*) and 3(*b*)(i), or by use of a small perfect crystal of the same dimensions (or nearly so) as the specimen crystal.

5. Discussion

In the classical mode, *i.e.* using one-dimensional profile measurement, the determination of a reflectivity distribution (referred to earlier as a rocking curve) required the use of a two-crystal spectrometer (see Compton & Allison, 1935; James, 1948). Even so, the capabilities of that instrument in this respect are displayed only for a rather special combination of crystal and apparatus parameters. The necessary conditions for the derivation of a reflectivity distribution free of wavelength dispersion are that the spacings of the two crystals should be identical and that they should be in the parallel $(n, -n)$ configuration. These conditions place a considerable restriction on the practical application of this technique in that one requires a range of monochromator crystals of appropriate spacings if one wishes to explore the reflectivity distributions of a series of reflections from a given specimen over a wide range of θ. The ultimate precision (in angular terms) of this instrument operating in this mode is extremely high and ideally suited for the examination of crystals with low defect content. Operationally, it functions normally with extended-face crystals.

For imperfect crystals, the angular range of the reflectivity distribution is, by the nature of such specimens, greater than that of a perfect crystal and so the angular precision required to measure the former is less critical than for the latter. As a result, the improved $\Delta\omega$, $\Delta 2\theta$ technique can enable the determination of the reflectivity distribution for such specimens in a single-crystal configuration. For this configuration, there are no restrictions on θ and all reflections of significant intensity can be studied. In addition, no special conditions apply to the crystal specimen except that the volume irradiated should be small. As noted in the text, affine transformation according to $t = 1/2$ [Fig. 2(*b*)(ii)] disposes the r^*/μ^* and λ loci at right angles. In effect, this provides a record of the reflectivity distribution over the range of the wavelength band of the measurement (~0·012 Å in this case), the minimum $\Delta\lambda$ band being that associated with the resolution capability of the set-up parallel to λ. In this case, it corresponds to 0·02–0·03°, this being determined by the size of the detector aperture convoluted with the size of the source. This is smaller than the α_1, α_2 separation, even at ~6·1°θ (~0·04°). So, in theory, one can inspect $r^*(\Delta\omega)$'s variation with λ and, if constant, then a more precise estimate of the average distribution can be derived.

The similarity of the disposition in $\Delta\omega$, $\Delta 2\theta$ space, appropriately transformed, of r^* and λ in the single-crystal configuration (for all θ) with that in the two-crystal configuration (only for $\theta_C = \theta_M$) can be seen by comparing Fig. 2(*b*)(ii) here and Fig. 8(*c*)(iii) of Mathieson (1985), which deals with small-crystal X-ray diffractometry with an ante-monochromator.

Investigation of the reflectivity (rocking) curve by means of the $\Delta\omega$, $\Delta 2\theta$ technique in conjunction with a 'tall thin' source is applicable not only to small single crystals but also to selected-area studies of extended-plate crystals (in transmission mode). While demonstrated here with a conventional X-ray tube source, the technique is obviously applicable with other radiation sources that can provide the necessary dimensional conditions, such as γ-rays and synchrotrons.

We are grateful to Dr H. J. Whitfield for the crystals of $CuInSe_2$. One of us (AWS) acknowledges the financial support of a CSIRO Postdoctoral Award.

APPENDIX

Practical point

The set-up that we have used in these experiments was not designed for the highest-resolution capability. The diffractometer is an early (1966) Picker, updated in respect of drives to axes and under computer control, but the essential mechanical features are unchanged. However, to extract the best out of any given combination of specimen crystal and detector aperture, a relatively simple adjustment is possible to 'match' the source size to the specimen/aperture combination. With the 'tall' source and an initial tube angle of tilt (take-off angle) of (say) 1 in 10, it was found that the α_1 peak signal overflowed the detector aperture (or pixel) used (~0·1 mm or ~0·02° wide). By decreasing the take-off angle of the X-ray tube, the $\Delta 2\theta$ spread of the peak signal will decrease but the signal within the aperture (pixel) remains essentially constant until the point when it contracts within the aperture and the signal level recorded by the detector will drop. It is in this region of adjustment that the 'match' is achieved. In our own case (with source-to-crystal and crystal-to-detector distances of approximately 20 and 25 cm respectively), we found this to be at ~3°, *i.e.* a tilt of 1 in 20. Since we are using a semi-microfocus tube whose focus is nominally 0·4–0·5 mm wide, this suggests an

optimum effective source size in the diffraction plane of ~25 μm.

The data presented in this paper, for the $\bar{1}\bar{1}2$ reflection of $CuInSe_2$, were collected using a take-off angle of 4° or approximately 1 in 14. Reflectivity curves for the $\bar{1}\bar{1}2$ reflection have also been derived from data collected with a take-off angle of 2° or approximately 1 in 30, using Mo $K\beta$, Mo $K\alpha$ and Cu $K\alpha$ unfiltered radiations. These r^*/μ^* distributions are very similar in shape to that in Fig. 3(*c*), the lowest FWHH being ~1·6′.

References

ALEXANDER, L. E. & SMITH, G. S. (1962). *Acta Cryst.* **15**, 983-1004.

ARNDT, U. W. & WILLIS, B. T. M. (1966). *Single Crystal Diffractometry.* Cambridge Univ. Press.

BRAGG, W. H. (1914). *Philos. Mag.* **27**, 881-899; reprinted in *Acta Cryst.* (1969), A**25**, 3-11.

COCHRAN, W. (1969). *Acta Cryst.* A**25**, 95-101.

COMPTON, A. H. & ALLISON, S. K. (1935). *X-rays in Theory and Experiment.* New York: Van Nostrand.

DARWIN, C. G. (1922). *Philos. Mag.* **43**, 800-829.

JAMES, R. W. (1948). *Optical Principles of the Diffraction of X-Rays.* London: G. Bell and Sons.

LOSHMANOV, A. A., CHERNYSHEVA, M. A., TRUNOV, V. A., KURBAKOV, A. I., SHALDIN, YU. V., SIZOVA, N. L., KUZMINA, I. P. & REGEL, V. R. (1984). *Cryst. Res. Technol.* **19**, 73-78.

MATHIESON, A. MCL. (1979). *Acta Cryst.* A**35**, 50-57.

MATHIESON, A. MCL. (1982). *Acta Cryst.* A**38**, 378-387.

MATHIESON, A. MCL. (1983*a*). *J. Appl. Cryst.* **16**, 257-258.

MATHIESON, A. MCL. (1983*b*). *Aust. J. Phys.* **36**, 79-83.

MATHIESON, A. MCL. (1983*c*). *J. Appl. Cryst.* **16**, 572-573.

MATHIESON, A. MCL. (1983*d*). *Acta Cryst.* A**39**, 79-83.

MATHIESON, A. MCL. (1984*a*). *Acta Cryst.* A**40**, 355-363.

MATHIESON, A. MCL. (1984*b*). *J. Appl. Cryst.* **17**, 207-209.

MATHIESON, A. MCL. (1985). *Acta Cryst.* A**41**. In the press.

MATHIESON, A. MCL. & STEVENSON, A. W. (1984). *Aust. J. Phys.* **37**, 657-665.

SCHNEIDER, J. R., HANSEN, N. K. & KRETSCHMER, H. (1981). *Acta Cryst.* A**37**, 711-722.

YELON, W. B., ALKIRE, R. W., SCHEIBER, M. M., VAN DEN BERG, L., RASMUSSEN, S. E., CHRISTENSEN, H. & SCHNEIDER, J. R. (1981). *J. Appl. Phys.* **52**, 4604-4609.

YELON, W. B., VAN LAAR, B., KAPRZYK, S. & MANIAWSKI, F. (1984). *Acta Cryst.* A**40**, 16-23.

Acta Cryst. (1985). A**41**, 296-301

Transferability of Nonbonded Cl···Cl Potential Energy Function to Crystalline Chlorine

BY DONALD E. WILLIAMS AND LEH-YEH HSU

Department of Chemistry, University of Louisville, Louisville, Kentucky 40292, *USA*

(*Received* 9 *July* 1984; *accepted* 9 *January* 1985)

Abstract

The crystal structure of molecular chlorine could not be accurately predicted using a transferred nonbonded Cl···Cl potential function that was found satisfactory for prediction of perchlorohydrocarbon crystal structures. Additional consideration of quadrupole-quadrupole interaction did not resolve this problem. One possible solution, which has been explored in the literature, was to define a new, nontransferable, Cl···Cl potential function specifically tailored to molecular chlorine. Such a specialized Cl···Cl function required additional adjustable parameters that defined an anisotropic nonbonded energy function for chlorine. A second possible approach, explored here, transferred the perchlorohydrocarbon Cl···Cl potential function to molecular chlorine. This simple isotropic nonbonded energy function was then supplemented by a partial intermolecular bonding force constant, which was applied to the short contacts present in this structure type. The resulting empirical model described the crystal structure of molecular chlorine within threshold accuracy.

Introduction

The heavier halogens Cl_2, Br_2 and I_2 have similar crystal structures with space-group symmetry *Cmca*. A summary of the crystal data is given in Table 1, and the structure type is illustrated in Fig. 1. Table 2 gives a summary of the observed lattice energies, and also the intramolecular bond distances and energies of the isolated molecules. The fact that these structures are layered, with all atoms in planes parallel to (100), immediately suggests that these are not simple van der Waals type structures. This is true because a normal van der Waals interaction would lead to a nonplanar type of molecular packing where the ends of the molecules in one layer are placed in staggered positions between the ends of molecules in the adjacent layer.

English & Venables (1974) have presented a general discussion of the crystal packing of diatomic molecules. They made a systematic study of several possible space groups for the packing of H_2, N_2, O_2, F_2, Cl_2, Br_2 and I_2 molecules in the crystal. One of their conclusions was that intermolecular bonding

0108-7673/85/030296-06$01.50